

## Atomic Structure of Core-Shell Precipitates in Al-Li-Sc-Zr Alloys Studied by Analytical and Aberration-Corrected TEM/STEM

M.D. Rossell,\* R. Erni,\* A. Tolley,\*\* E. Marquis,\*\*\* V. Radmilovic,\* and U. Dahmen\*

\* National Center for Electron Microscopy, Lawrence Berkeley National Laboratory, University of California, 1 Cyclotron Road, Berkeley, CA 94720, USA

\*\* Centro Atómico Bariloche, CNEA, CONICET, 8400 San Carlos de Bariloche, Argentina

\*\*\* Department of Materials, Oxford University, Parks Road, Oxford OX1 3PH, UK

The current interest in ternary Al-Sc-Zr alloys [1-3] arises from their ability to form small ordered dispersoids which effectively increase the alloy's resistance to plastic deformation and recrystallization. These coherent precipitates were found to consist of an Al<sub>3</sub>Sc core surrounded by a Zr-rich shell. Here we report on the structure of new core-shell precipitates that can be formed by adding Li to Al-Sc-Zr.

Energy-filtered, conventional high-resolution as well as aberration-corrected TEM/STEM was used to study the atomic structure of these core-shell precipitates. For aberration-corrected microscopy we employed the TEAM 0.5 instrument [4], a double-C<sub>s</sub>-corrected microscope with a hexapole aberration corrector in the imaging part that fully corrects aberrations up to third order and partially up to fifth order, and an improved hexapole aberration corrector for the probe that fully corrects aberrations up to fifth order with an information transfer to 0.05 nm. The enhanced chemical sensitivity of this instrument allowed us to clearly image atomic columns of Li using exit wave reconstructions. In addition, atom-probe tomography (APT) was used to study the precipitates and in particular to deduce the chemical composition of the different phases present.

A conventional high-resolution electron micrograph of one of these Al<sub>3</sub>(LiScZr) precipitates formed after a heat treatment of 18h at 450°C followed by 4h at 190°C is shown in Figure 1A. In projection, the precipitate exhibits a doughnut shape with a high intensity shell surrounding a core region whose contrast closely resembles the Al matrix. Energy filtered jump ratio maps of Li and Sc (Figures 1B and 1C, respectively) indicate that Sc is confined to the core while Li is primarily located at the shell, though some Li is also found in the core. The aberration-corrected high-angle annular dark field (HAADF) scanning transmission electron micrograph of the core/shell interface in Figure 1D confirms that the core region exhibits an L1<sub>2</sub> order with the bright Sc atom columns defining a square pattern.

The chemical composition as deduced from APT of the core region is Al<sub>3</sub>(Li<sub>0.40</sub>Sc<sub>0.48</sub>Al<sub>0.12</sub>) (Figure 2A). For this composition, the mean atomic scattering factor of the B=Li,Sc,Al sublattice in the fully ordered A<sub>3</sub>B structure is very similar to that of Al and thus leads to vanishing superlattice reflections. Pendellösung plots of the intensity of the 200, 220, 100 and 110 diffracted beams as a function of thickness and calculated dynamical selected area diffraction patterns (SADP) along the [001] zone axis for Al, Al<sub>3</sub>(Sc<sub>0.48</sub>Li<sub>0.40</sub>Al<sub>0.12</sub>) and Al<sub>3</sub>Li are shown in Figures 2C-2H, respectively. The intensity of the characteristic 100 and 110 L1<sub>2</sub> superlattice reflections falls to zero for a core composition Al<sub>3</sub>(Li<sub>0.40</sub>Sc<sub>0.48</sub>Al<sub>0.12</sub>) (Figure 2D and 2G), resembling the Al matrix (Figure 2C and 2F), unlike the Al<sub>3</sub>Li shell (Figure 2E and 2H).

We retrieved the exit-plane wave function of one of the precipitates from a focal series recorded on the aberration corrected instrument. The phase of the reconstructed exit plane wave in Figure 2B reveals the  $\text{Al}_3\text{Li}$  long range order where Al columns can be clearly distinguished from Li columns. By comparison, in the core the long range order is not directly observable as it is in HAADF STEM. These observations demonstrate the increased sensitivity of aberration-corrected microscopy and the complementary nature of TEM and STEM imaging modes.

## References

- [1] A. Tolley et al., *Scripta Mater.* 52 (2005) 621.
- [2] C.B. Fuller et al., *Acta Mater.* 53 (2005) 5415.
- [3] E. Clouet et al., *Nature Materials* 5 (2006) 482.
- [4] The TEAM project is supported by the U.S. Department of Energy, Office of Science.

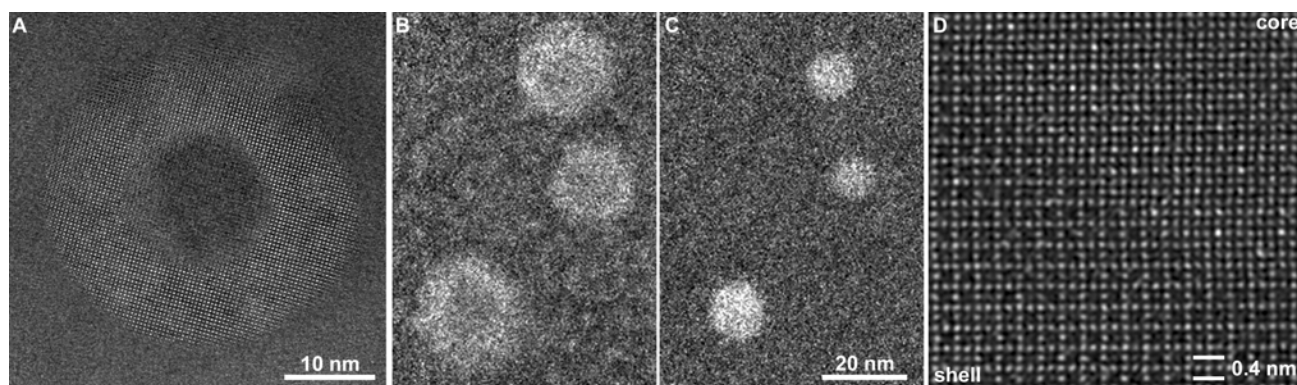


FIG. 1. A. [001] HREM image of an  $\text{Al}_3(\text{LiScZr})$  core/shell precipitate. B,C. Energy filtered jump ratio maps of three core/shell precipitates showing Li and Sc distribution, respectively. D. Low-pass filtered HAADF image of the core/shell interface along the [001] zone axis

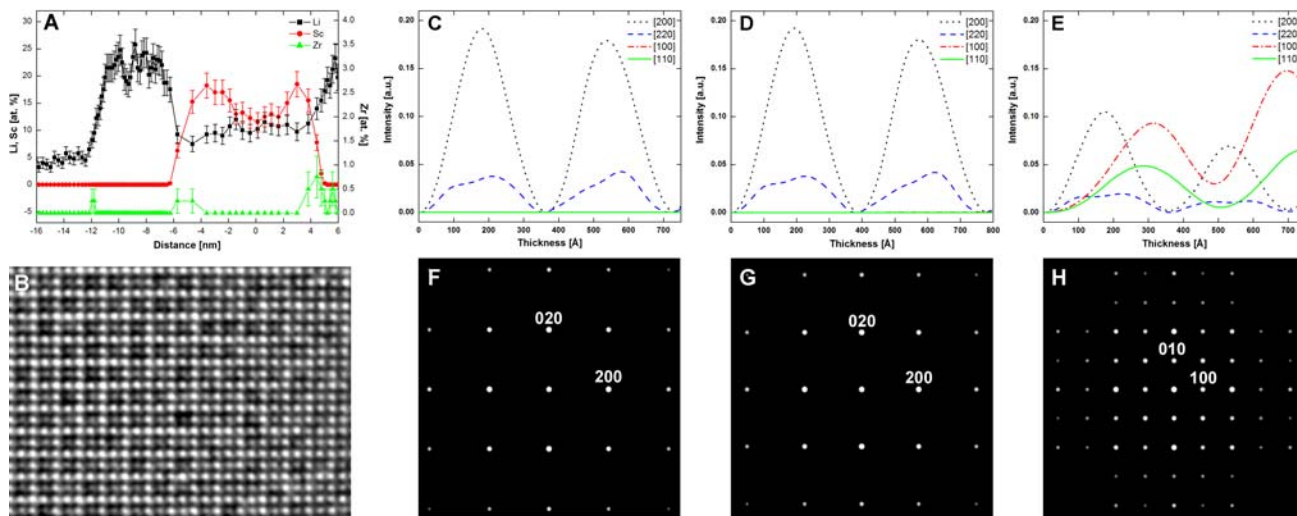


FIG. 2. A. APT concentration profile across a core/shell particle. For clarity, the zero position has been placed at the center of the core. B. Experimental  $\text{Al}_3\text{Li}$  exit wave phase image in the [001] zone axis, reconstructed from 20 experimental images. The  $\text{Al}_3\text{Li}$  unit cell measures 0.4 nm. C-H. Pendellösung plots of the intensity of the 200, 220, 100 and 110 diffracted beams as a function of thickness, and corresponding calculated dynamical SADP along the [001] zone axis for a specimen thickness 150 Å for (C,F) Al, (D,G)  $\text{Al}_3(\text{Sc}_{0.48}\text{Li}_{0.40}\text{Al}_{0.12})$  and (E,H)  $\text{Al}_3\text{Li}$ .